Bioresource Technology 236 (2017) 129–137

Contents lists available at ScienceDirect

Bioresource Technology

journal homepage: www.elsevier.com/locate/biortech

Co-liquefaction of mixed culture microalgal strains under sub-critical water conditions

Kodanda Phani Raj Dandamudi [a,e], Tapaswy Muppaneni [a,e], Nilusha Sudasinghe [b,f], Tanner Schaub [b], F. Omar Holguin [c], Peter J. Lammers [d], Shuguang Deng [a,e,*]

[a] Chemical Engineering Department, New Mexico State University, Las Cruces, NM 88003, USA
[b] Chemical Analysis and Instrumentation Laboratory, New Mexico State University, Las Cruces, NM 88003, USA
[c] Plant and Environmental Sciences, New Mexico State University, Las Cruces, NM 88003, USA
[d] School of Sustainable Engineering and the Built Environment, Arizona State University, Tempe, AZ 85287, USA
[e] School for Engineering of Matter, Transport and Energy, Arizona State University, Tempe, AZ 85287, USA
[f] Bioscience Division, Los Alamos National Laboratory, Los Alamos, NM 87545, USA

HIGHLIGHTS

- Co-liquefaction of micro-algae has alleviated the biocrude oil yield at similar reaction conditions.
- Positive synergistic effect was observed during the co-liquefaction of micro-algae.
- Detailed compositional analysis of biocrude oil produced by individual and co-liquefied micro-algae.
- First application of APPI FT-ICR MS to algal HTL biocrude oils.
- The HHV of biocrude oil produced by co-liquefaction of micro-algae was 35.28 MJ/kg.

GRAPHICAL ABSTRACT

Abundance contour plots of biocrude oils obtained at 300 °C.

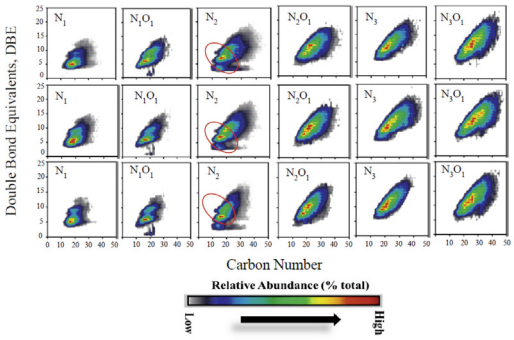

ARTICLE INFO

Article history:
Received 16 January 2017
Received in revised form 22 March 2017
Accepted 28 March 2017
Available online 29 March 2017

Keywords:
Hydrothermal liquefaction
Co-liquefaction
Synergistic effect
FT-ICR MS
Microalgae

ABSTRACT

We report the co-liquefaction performance of unicellular, red alga *Cyanidioschyzon merolae* and *Galdieria sulphuraria* under sub-critical water conditions within a stainless-steel batch reactor under different temperatures (150–300 °C), residence time (15–60 min), and *Cyanidioschyzon merolae* to *Galdieria sulphuraria* mass loading (0–100%). Individual liquefaction of *C. merolae* and *G. sulphuraria* at 300 °C achieved maximum biocrude oil yield of 18.9 and 14.0%, respectively. The yield of biocrude oil increased to 25.5%, suggesting a positive synergistic effect during the co-liquefaction of 80–20 mass loading of *C. merolae* to *G. sulphuraria*. The biocrude oils were analyzed by FT-ICR MS which showed that co-liquefaction did not significantly affect the distribution of product compounds compared to individual oils. The co-liquefied biocrude and biochar have a higher-heating-value of 35.28 and 7.96 MJ/kg. Ultimate and proximate analysis were performed on algae biomass, biocrude and biochar.

* Corresponding author at: School for Engineering of Matter, Transport and Energy, Arizona State University, Tempe, AZ 85287, USA.
E-mail address: shuguang.deng@asu.edu (S. Deng).

http://dx.doi.org/10.1016/j.biortech.2017.03.165
0960-8524/

1. Introduction

As the interest for vitality strengthens in the midst of developing attentiveness toward extreme environmental change, biofuels are required like never as a contrasting option to fossil powers. Recently, expanding considerations are being paid to the usage of biofuels because of their renewability and net production of greenhouse gases. Among current feedstock candidates, microalgae are considered as a standout due to its ability to grow in a variety of environments, high photosynthetic efficiency, high area-specific yields. Additionally, microalgal cultivation production schema have the potential to effect waste water treatment systems (Brown et al., 2010; Pearce et al., 2016; Wang et al., 2010). Various technologies have been developed to extract and convert the dry algal biochemical constituents to fuel precursors but have issues of higher power demand, energy costs due to drying and utilize lipid-only portion of available biomass (Demirbas, 2010; Patil et al., 2008; Williams and Laurens, 2010). Hence, the necessity of producing biofuels from wet biomass, without drying and to utilize whole algal biomass is of growing interest.

Among such developed technologies, Hydrothermal liquefaction (HTL) method is growing attention due to its ability to convert biomass with very high water contents at higher temperatures and pressures to produce an aqueous, biocrude, solid residue and a gaseous fraction (Toor et al., 2011). During HTL, the catalytic and solvating properties of water are enhanced to degrade biomacromolecules involving dehydration, decarboxylation and deamination to re-polymerize into energy-dense oily compounds (Biller and Ross, 2011; Zhang et al., 2010). Literature provides reports on HTL of microalgae using with/without catalysts (Ross et al., 2010), co-liquefying with coal, polymers, swine and mixed-culture strains (Chen et al., 2014; Ikenaga et al., 2001; Jin et al., 2013). These studies suggested that the co-liquefaction of biomass with mentioned materials has alleviated the conversion and enhanced the quality and quantity of biocrude yield. This could be due to the catalytic effect of chemical compounds present in biomass to aid in the degradation of bio-macromolecules and thus exhibit positive synergistic effect. In addition to interest for identifying fuel-specific algal strains, cultivation of those monocultures in an industrial-scale process is challenging due to culture crashes from diseases, climatic disturbances and contamination by invasive species and other organisms (bacteria and other microorganisms) (Godwin et al., 2017; Xu et al., 2009); mainly in waste water-integrated algal production facilities. Therefore, it is highly critical in identifying and selecting algal strains that can tolerate and grow in similar conditions. *Cyanidioschyzon merolae* and *Galdieria sulphuraria* and the mixture of two species were selected in this study to run under subcritical water conditions and investigate the quantitative and qualitative performance of mixed microalgal strains. *C. merolae* & *G. sulphuraria* are unicellular, thermotolerant acidophilic red alga adapted to grow in extreme conditions (pH 0.5–4, 56 °C) (Muppaneni et al., 2017; Selvaratnam et al., 2014). Jin et al. (2013) have evaluated the effect of co-liquefaction of micro- and macro-algae in subcritical water conditions and reported a positive synergistic effect.

Hydrothermal liquefaction involves a series of multicomponent reactions that convert mainly carbohydrates, lipids and proteins resulting in the complex biocrude mixtures (Bobleter, 1994; Chiaberge et al., 2014). The previous studies on analysis of hydrothermally liquefied algal biocrude oils by GC–MS, 1H NMR reveals the presence of fatty acids (C14-C20), long-chain hydrocarbons (C17-C22), aromatic and polar compounds, such as oxygen and nitrogen-containing compounds (Muppaneni et al., 2017; Roberts et al., 2013; Zhou et al., 2010). Fourier transform ion cyclotron resonance mass spectrometry (FT-ICR MS) has been widely used for the compositional analysis of mixtures with high complexity owing to its ultra-high mass resolving power and high mass measurement accuracy (Christensen et al., 2015; Schaub et al., 2008; Sudasinghe et al., 2014). In the current study, both positive-, negative-ion electrospray ionization (ESI) and positive-ion atmospheric-pressure photoionization (APPI) FT-ICR MS techniques were employed to characterize complex mixture of algal HTL biocrude oils. Each ionization technique has specific target analytes based on molecular-weight, polarity and chemical properties. The integration of data from multiple ionization techniques results in the detection of wide range of compounds, thus providing a baseline description of the composition of the biocrude oils.

2. Materials and methods

2.1 Materials

The performance of two microalgal strains under similar HTL conditions was assessed in this study. *Cyanidioschyzon merolae* (*C. merolae* MS1-YNP) (Toplin et al., 2008) and *Galdieria sulphuraria* (*G. sulphuraria* CCMEE 5587.1) (Selvaratnam et al., 2015), two individual strains of acido-thermophilic unicellular red alga species obtained from the Culture Collection of Microorganisms from Extreme Environments (Pacific Northwest National Laboratory, Richland, U.S.A.) were used in this study. Standard cyanidium media modified to contain twice the concentration of ammonium sulfate and supplemented with the vitamin component of f/2 algal medium (Andersen, 2005) was supplied in an incubator as growth media for both the strains at 40 °C with a 14 h/10 h light/dark cycle and CO_2 level maintained at 2–3% (vol/vol). The composition of modified cyanidium media was prepared as mentioned in (Selvaratnam et al., 2015). Single colonies were then separated from cultures streaked onto agar plates and scaled up to a volume of 1-L Erlenmeyer flasks containing modified Cyanidium media. These cultures were preadapted at 40 °C with a 14 h/10 h light/-dark cycle and left for 24 h to avoid adaptation-related issues. Following the preadaptation step, biomass used in the current study to produce HTL products were grown outdoors in a standard cyanidium medium in a temperature-controlled 4000-L outdoor horizontal photo bioreactor at New Mexico State University algal cultivation facility (Las Cruces, U.S.A) as described elsewhere (Selvaratnam et al., 2014). The chemicals, dichloromethane (DCM) and other solvents used in analysis were purchased from Sigma Aldrich, Saint Louis, MO, USA and used as received. Proximate analysis (ash and moisture) and biochemical analysis (lipids measured as FAME) of microalgae were determined per the procedures reported by (Muppaneni et al., 2017). The protein content of algae was calculated as 4.78 times the amount of nitrogen evolved during the elemental analysis of microalgae (Laurens et al., 2012). Ultimate analysis for algae, bio-crude and biochar was performed as mentioned in (Wang et al., 2015). High heating value (HHV) of the algae, biochar and bio-crude was determined using a bomb calorimeter (Parr Model 6725 Semi-micro Calorimeter). The analysis results of the biomass is listed in Table 1.

2.2. HTL experimental procedure

All the individual and co-liquefaction experiments were performed in a 100-ml stainless steel bench top reactor (Model 4593, Parr Instrument Company, Moline, IL) equipped with a magnetic stirrer, heater and a 4843-controller unit. In each experiment, a slurry of 50 g containing 10 g oven dry algae and rest as water were added into the reactor. The reactor was sealed and subsequently purged with nitrogen gas (99.98% pure), at least three times to remove all the residual air on top of the liquid mixture. An initial pressure of 2.3 MPa was maintained in the reactor during

all the experiments by adding nitrogen. The reactor was heated using an external heater controlled by controller at a heating rate of 10 °C/min and maintained at a desired reaction temperature and time. The reactor was then cooled to room temperature, vented and opened; 25 ml of dichloromethane (DCM) was added to the reaction vessel and mixed with the contents. The contents (liquid and solid mixture) were then transferred to glass separation funnel equipped with a filter paper to separate solid from the liquid fraction. The liquid fraction was allowed to phase separate and the bottom portion was decanted as DCM phase; the top portion as aqueous phase. The DCM phase is subjected to evaporation in a rotary evaporator at 65 °C under vacuum to recover the biocrude. The solid fraction was dried in an oven at 80 °C for >6 h and termed as biochar. All the biocrude; and aqueous fractions were stored (under ~5 °C) for further analysis. The yields of each product were calculated by dividing the mass of each fraction by the mass of oven dry algal biomass originally loaded into the reactor as mentioned in Valdez et al. (2012). HTL experiments were conducted by varying key operating parameters in between 150 and 300 °C with 50 °C interval, 30 min and 20 wt.% for reaction temperature, reaction time and total solid ratio, respectively. Co-liquefaction of microalgae was performed at *C. merolae* / *G. sulphuraria* mass ratio of 0–100%; at maximum yield point (300 °C and 80–20% *C. merolae*/*G. sulphuraria* mass ratio) experiments were also performed at solid loading (5–20%), time (30–60 min). Triplicate runs were performed at nominally similar conditions and mean values were reported in the results (Table 2).

2.3. FT-ICR mass spectrometry

A concentration of 3 mg/mL stock solution was prepared by dissolving the HTL biocrude samples in 1:1 chloroform: methanol. For positive-ion ESI (electrospray ionization) FT-ICR mass spectral analysis, the stock solution was diluted 10-fold with 1:2:4 chloroform: methanol: 2-propanol containing 0.1% formic acid as an ESI modifier. A 20-fold dilution of stock was performed in negative-ion mode ESI analysis, by adding 2:1:1 acetonitrile: methanol: water containing 0.1% ammonium hydroxide. For positive-ion APPI (atmospheric pressure photoionization) analysis the same stock solution was diluted 50-fold with toluene to analyze the non-polar components present in the biocrude samples. No fragmentation of the peaks was observed in the spectra as confirmed by using the internal standard, naphtho [2,3-a]pyrene. All the biocrude samples were filtered to remove suspended solids using an Acrodisc CR 13 mm syringe filters with 0.2 μm PTFE membranes prior to analysis. ESI and APPI FT-ICR mass spectrometry was performed on the final dilute biocrude samples with a hybrid linear ion trap 7 T FT-ICR mass spectrometer (LTQ FT, Thermo Fisher, San Jose, CA). The prepared samples were directly infused using an Advion Triversa Nanomate (Advion, Ithaca, NY); and with a syringe pump (Hamilton) at a flow rate of 50 μL/min in ESI and APPI modes respectively. A total of 500 and 350 time-domain transients were co-added in ESI (both positive and negative modes) and APPI mode, respectively prior to fast Fourier transformation and frequency to *m*/*z* conversion.

Table 1
Analysis of algal feedstock.

Species	*C. merolae*	*G. sulphuraria*
Proximate (wt.%)		
Ash	10.0 ± 1.5	9.4 ± 0.89
Moisture	53.73 ± 1.5	67.35 ± 2.0
Biochemical (wt.%)		
Lipids	4.35 ± 0.91	3.21 ± 0.55
Proteins	47.8 ± 1.6	45.1 ± 1.1
Carbohydrates[a]	37.85	42.29
Ultimate (wt.%)		
C	48.13	42.4
H	5.14	3.9
N	9.99	9.41
S	1.24	1.36
O[a]	35.5	42.93
HHV (MJ kg^{-1})	18.11	16.4

[a] Calculated by difference; HHV: high heating value.

Table 2
Elemental composition of bio-crude oils and biochar obtained at 300 °C.

	C	H	N	S	O[a]	HHV, MJ/kg
Biocrude oil						
C. merolae	78.07	6.45	3.75	0.90	10.83	33.84
G. sulphuraria	76.62	8.16	6.24	1.67	7.31	36.45
Q (80–20 wt.%)	74.20	8.06	7.68	1.33	8.73	35.28
Biochar						
C. merolae	49.1	5.39	4.18	0.84	40.49	17.16
G. sulphuraria	54.92	7.24	3.26	0.87	33.71	23.02
Q (80–20 wt.%)	34.26	4.37	4.97	0.9	55.5	7.96

[a] Calculated by difference; HHV: high heating value.

3. Results and discussion

This section provides information about influence of temperature, biomass loading and time on product yields from each HTL reaction condition, along with the molecular and elemental characterization of the biocrude phase from various experiments. Various forms of results for biocrude samples from FT-ICR MS analysis include isoabundance contour plots, hetero atom class distribution in both ESI (positive-, and negative-ion modes) and APPI techniques.

3.1. Analysis of feedstock

Table 1 shows the proximate, ultimate and biochemical composition of the two microalgal feedstocks. The lipid content of the two microalgal strains is considerably low, around 3–5%. The relatively higher nitrogen content in *C. merolae* has an influence on its higher protein content (~48%). *G. sulphuraria* on the other hand has higher range of carbohydrates (~42%) which corresponds to its lesser lipid and protein values. Ultimate analysis of microalgae reveals that both have similar content of sulphur, and oxygen content was 35.5 and 43.0% for *C. merolae* and *G. sulphuraria*, respectively. *C. merolae* has a higher value of HHV (18.11 MJ/kg) which corresponds to it less oxygen content.

3.2. Hydrothermal liquefaction (HTL) results

Literature studies indicate that HTL reaction temperature, biomass solid loading, and residence time were the influential factors in the yields of product fractions (Toor et al., 2013; Anastasakis and Ross, 2011). These play a crucial role in defining the quality and quantity of the product fractions. Hence, the influence of various metrics was studied in the stainless-steel batch reactor.

3.2.1. Effect of reaction temperature on the product fraction yields

The HTL product fractions of algae include biocrude, biochar, water soluble components and incondensable gas. However, the yields of biocrude and biochar were emphasized in this current study. Product yields as a function of temperature from individual HTL of *C. merolae* and *G. sulphuraria* were presented on the dry weight basis in Fig. 1. Experiments were performed for individual species in the range of 150–300 °C, with an increment of 50 °C and a reaction time of 30 min and a solid loading of 20 wt.%. At

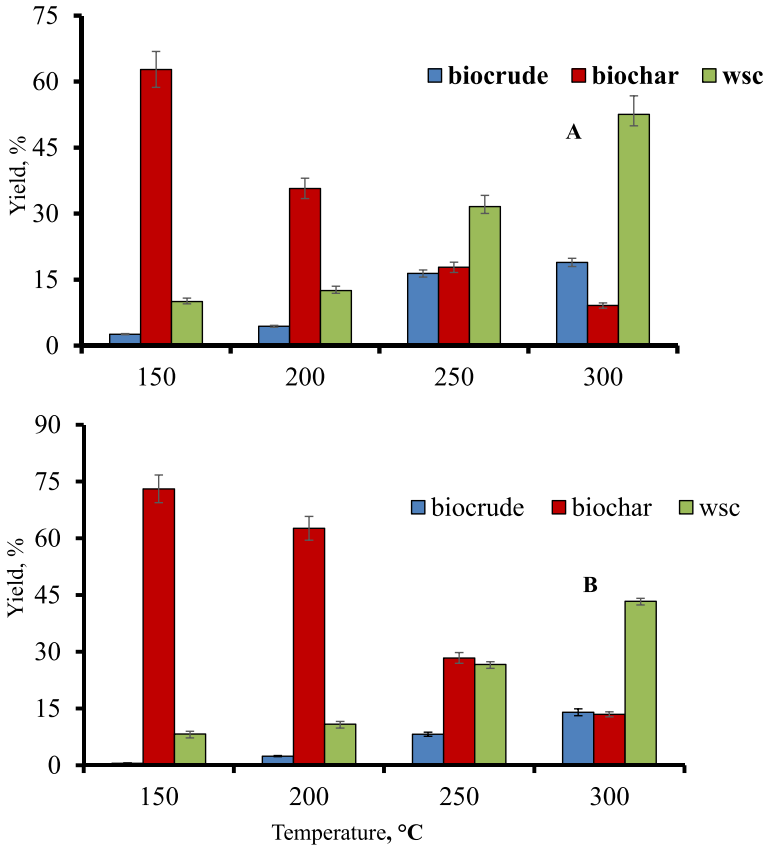

Fig. 1. Hydrothermal liquefaction product fraction yields with respect to temperature; (A) *C. merolae* at different HTL reaction temperatures; (B) *G. sulphuraria* at different HTL reaction temperatures.

150 °C, it can be clearly seen that biocrude yield was less than 3% (2.6 & 0.5% for *C. merolae* and *G. sulphuraria*, respectively) suggesting that there was minimal conversion of biomass into biocrude oil, similar to that of mentioned in Zhou et al. (2010). This was also explained with the highest biochar yields for both species (62.8 & 73.0% for *C. merolae* and *G. sulphuraria*, respectively) at reaction temperature of 150 °C. Therefore, further experiments were performed at 200 °C and an increment of biocrude oil yield was observed (4.4 & 2.4% for *C. merolae* and *G. sulphuraria*, respectively), suggesting that increase in temperature would be responsible for biocrude oil yield increase. It is evident that a 4-fold increase in biocrude oil yield was observed (16.4 & 8.2% for *C. merolae* and *G. sulphuraria*, respectively) when the reaction temperature was increased from 200 to 250 °C, suggesting the degradation of biomass is favored toward the formation of biocrude phase. Upon increase in temperature to 300 °C the biocrude yield increased to 18.9 & 14.0% for *C. merolae* and *G. sulphuraria*, respectively. Similar trend of HTL yields for biocrude was observed in Yu et al. (2011) and was evident that more biomass degradation and/or biocrude oil yield was temperature dependent and along with lipids other biochemical components are also converted to product phase. Lipids mainly comprising of triacylglycerides (TAG's) can be hydrolyzed under temperature sensitive conditions in order to fuel based molecules like free fatty acids and glycerol (Christensen et al., 2015; Toor et al., 2011). As mentioned in Table 1, the lipid contents of *C. merolae* and *G. sulphuraria* were 4.3 and 2.5%, respectively; indicating that non-lipid biochemical fraction of the cell including proteins and carbohydrates were also converted into biocrude phase, comparable with a study which communicated the trend for biocrude formation as lipids > proteins > carbohydrates (Biller and Ross, 2011). The yield of biochar followed an opposite trend of biocrude with decrease in yield from 62.8 to 9.2% and 73.0 to 13.4%, within the similar temperature range, suggesting that the increase in temperature has led to the conversion of organic matter in the biomass. With the observed trends of yields in the product phase, maximum yield of biocrude (18.9 and 14.0% for *C. merolae* and *G. sulphuraria*, respectively) was achieved at 300 °C for both species. Therefore, the optimal temperature for further co-liquefaction experiments was selected as 300 °C.

3.2.2. Effect of C. merolae to G. sulphuraria biomass loading on the yields of product fractions

As mentioned above, the selected optimal experimental conditions for co-liquefaction experiments were 300 °C, 30 min and a solid loading of 20 wt.%. A series of experiments varying *C. merolae*/*G. sulphuraria* biomass loading from 0 to 100% were performed. 100–0 and 0–100% represents the biocrude yields obtained from individual liquefaction of *C. merolae* and *G. sulphuraria*, respectively. 50–50 represents the ratio of *C. merolae* to *G. sulphuraria* mass loaded into the reactor (50% of *C. merolae* and 50% of *G. sulphuraria* constitute the mass of biomass in the HTL reactor). Experimental results were shown in Fig. 2 A and can be observed that biocrude yield of 16.5% at 50–50 and 13.0% at 20–80 solid loading was achieved. Interestingly, an increase in biocrude oil yield (25.5%) was observed at 80–20% *C. merolae* to *G. sulphuraria* ratio, suggests a positive synergistic and mutually enhancing effect during co-liquefaction of *C. merolae* to *G. sulphuraria* mixture. The maximum synergistic effect was obtained at a biomass ratio of 80–20 (*C. merolae*-*G. sulphuraria* respectively).

Current results from the co-liquefaction were in comparison and as mentioned to that of literature Jin et al. (2013), the fatty acids derived from one species promoted the conversion of organic matter into biocrude and thereby establishing a synergistic effect. To the best of our knowledge, literature provides no adequate

reports on co-liquefaction of mixed culture microalgal strains under sub-critical water conditions. However, the chemical compounds and the underlying mechanism involved in enhancing the yield needs to be investigated in further research endeavors. The biocrude yields and the synergetic effect decreased with further increasing in solid loading ratio, implying that the rational ratio was about 80–20 wt.% (hereafter referred as Q); where the highest yield was achieved.

3.2.3. Effect of time on the yield of HTL product fractions

As mentioned earlier, after fixing the optimum ratio for co-liquefaction to be Q at 300 °C, 30 min and solid loading of 20 wt.%; series of HTL tests were performed to study the influence of residence time on the product yield at Q. Fig. 2 B depicts the trend of biocrude oil yield as a function of time. Experiments were conducted in the range of 15–60 min with 15 min interval and was observed that the biocrude yield increased markedly by ~5% within the first interval from 15 min to 30 min. The swift increase in the biocrude yield can be due to the cell lysis subjected to temperature and pressure differentials in and around the cell during reaction (Faeth and Savage, 2016; Garcia Alba et al., 2011). The maximum biocrude yield was observed at 30 min and further increase in time has no positive influence on the biocrude yields and was similar to that of Yang et al. (2016). Accordingly, the yield of biochar declined from 25.6 to 12.4% during the above-mentioned duration. Further increase in the reaction time have increased the biochar yield possibly due to condensation, subsequent cracking and/or re-polymerization reactions of the reactive components in the biocrude (Jin et al., 2013) and have started to level off at a residence time of 60 min.

3.3. FT-ICR MS analysis of biocrude

A thorough compositional analysis of biocrude oils produced from individual and co-liquefied HTL process was performed by ESI and APPI FT-ICR mass spectrometry. FT-ICR MS affords ultra-high mass resolving power (i.e. $m/\Delta m_{50\%} = 400{,}000$ at m/z 400, where $\Delta m_{50\%}$ is the mass spectral peak width at half-maximum peak height) and sub-ppm level mass measurement accuracy that enables a complete compositional characterization of highly complex mixtures. The mass spectra collected from the biocrude samples seemed to be complex with many peaks in all the above-mentioned techniques owing to numerous compounds in HTL biocrude oil. All the peaks were generated with S/N of 10 or more and on average more than 750 peaks have been identified.

3.3.1. ESI FT-ICR mass spectrometry

The HTL biocrude oils produced by the individual HTL of *C. merolae* and *G. sulphuraria* at 150–300 °C, solid loading of 20 wt.% and 30 min residence time were analyzed by ESI FT-ICR MS and the hetero atom class distribution for HTL biocrude in both positive- and negative-ion modes is shown in Fig. 3. Basic nitrogen compounds with oxygen number varying from 0 to 3 represent the dominant classes in positive-ion mode ESI for both microalgal species. As seen from the Fig. 3 A and B, N_2 is the most abundant class in 300 °C biocrude oil sample and its relative abundance decreases with decrease in temperature. Increase of the oxygen atom number to the nitrogen compound class also decreases its abundance with decrease in temperature. The increase in the abundance of nitrogenous compounds with temperature suggests the degradation of non-lipid components (e.g. proteins and carbohydrates) into

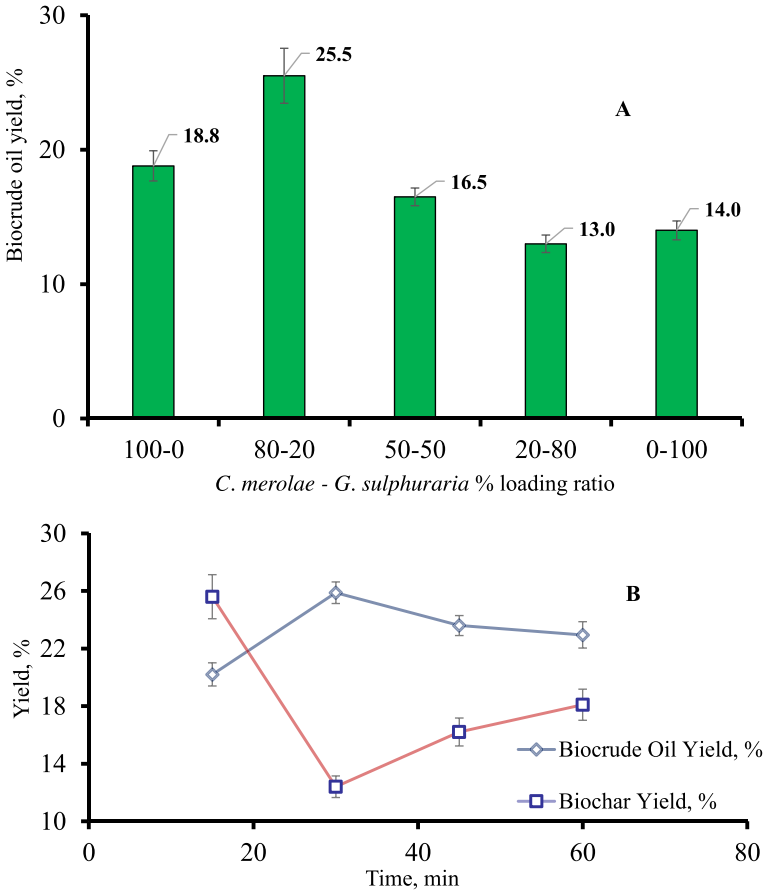

Fig. 2. Top (A) HTL biocrude yield on co-liquefaction of *C. merolae* & *G. sulphuraria* at 300 °C; Bottom (B) Biocrude and biochar yield on co-liquefaction of *C. merolae* & *G. sulphuraria* at Q with respect to time.

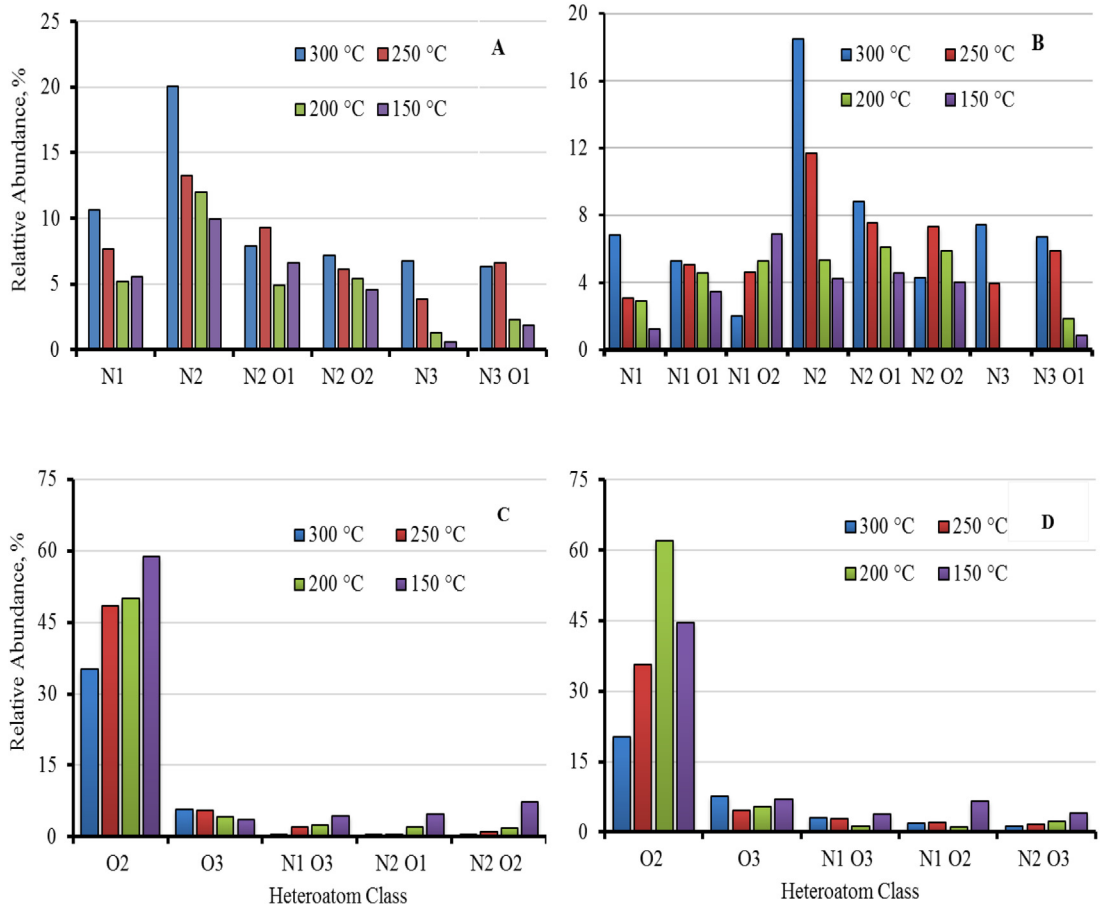

Fig. 3. Positive- and negative-ion ESI heteroatom class distributions for biocrude oils produced from pure *C. merolae* and *G. sulphuraria* at different reaction temperatures; Top (A), (+) ESI heteroatom class analysis of biocrude oils generated from *C. merolae*; Top (B), (+) ESI heteroatom class analysis of biocrude oils produced from *G. sulphuraria*; Bottom (C), (−) ESI heteroatom class analysis of biocrude oils from *C. merolae*; Bottom (D), (−) ESI heteroatom class analysis of biocrude oils from *G. sulphuraria*.

biocrude oil (Torri et al., 2012). Mono-, and di-nitrogen classes showed a steady increase in abundance with increase in HTL temperature in both algal species. The increase in the HTL temperature from 150 to 300 °C has shown an increase in the abundance of di-nitrogen (N_2) species by ~2-fold, and ~4-fold for *C. merolae* and *G. sulphuraria*, respectively. Nitrogenous compounds mostly arise due to the degradation of proteins at higher temperature and were directly responsible for the increase in the HTL biocrude oil yield with temperature. The observed nitrogen-containing compounds in the positive ion mode could possibly correspond to pyridinic compounds (Sudasinghe et al., 2014).

Fig. 3 C and D shows the negative-ion ESI FT-ICR MS hetero atom class distribution of biocrude oils produced from the liquefaction of *C. merolae* and *G. sulphuraria* at different reaction temperatures. Among, the acidic species, O_2 was the dominant class observed for both algal species biocrude oils produced at different temperatures. It was observed that the intensity of the O_2 class increases with a decrease in temperature. Other classes identified in the negative-ion mode include O_x ($x > 2$) and $N_{1\text{-}2}O_x$. This wide range of oxygenated compounds observed in this mode may be due to the degradation of lipids and carbohydrates during the thermochemical process. Acidic nitrogen containing compounds (e.g. pyrrolic compounds) can be observed due to their selective ionization in negative mode. The classes observed were consistent with HTL of bio-oil and residual water soluble organics analyzed by FT-ICR MS (Sudasinghe et al., 2014).

Heteroatom class distribution of co-liquefied biocrude oils obtained at Q in both positive-ion mode (Top) and negative-ion mode (Bottom) FT-ICR MS are presented in Fig. 4 A and B, respectively. Primary classes observed in the positive-ion mode were N_1, N_2, N_3, N_3O_1, N_2O_2 suggesting the degradation of carbohydrates and proteins along with secondary reaction products. Fig. 4 B shows that the dominant classes observed in negative-ion mode FT-ICR MS were O_2, O_3, N_2O_3, N_2O_2, N_1O_3, and N_1O_2 that originate from the free fatty acid of the lipid portion. The molecular composition of biocrude oils remains largely the same despite co-liquefaction, where co-liquefied biocrude oils produced at Q show similar abundant compounds to those of individual HTL oils produced at higher temperature. Positive-ion ESI FT-ICR MS abundance-contoured plots of Double Bond Equivalents (DBE) vs carbon number for the abundant basic nitrogen species observed for the biocrude oils produced by individual- (300 °C) and co-liquefaction (Q) are shown in Fig. 5. The N_2 species for the three biocrude oils show 3–20 DBE and carbon content of ~10–40 atoms. These compounds could correspond to long-chain diamines, alkyl-substituted imidazoles, and/or alkylated pyrazines as reported in Sudasinghe et al. (2014). All the three biocrude oils shows high abundance compositional regions for the N_2 class at DBE = 6–9 and carbon number = 14–20. Similar results have been observed for the other classes including N_1 and N_1O_1. Therefore, co-liquefaction of microalgae enhanced the biocrude oil yield with no effect on the molecular composition but affected the relative amount of individual component in the biocrude oil.

3.3.2. APPI FT-ICR mass spectrometry

Atmospheric pressure photoionization coupled with FT-ICR MS produces ions for moderately-polar and non-polar species that are not ionized by ESI. It efficiently ionizes nonpolar compounds and

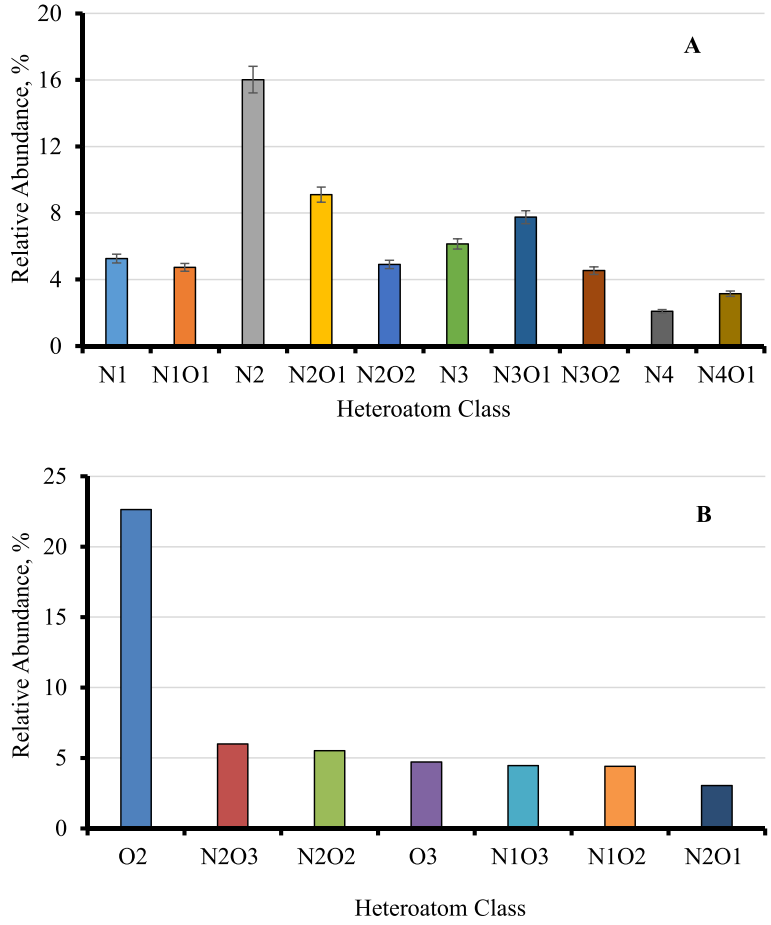

Fig. 4. Heteroatom class distribution of co-liquefied bio-crude oil; Top (A), (+) mode ESI heteroatom class distribution of co-liquefied oil at Q; Bottom (B), (−) mode ESI heteroatom class of co-liquefied oil at Q.

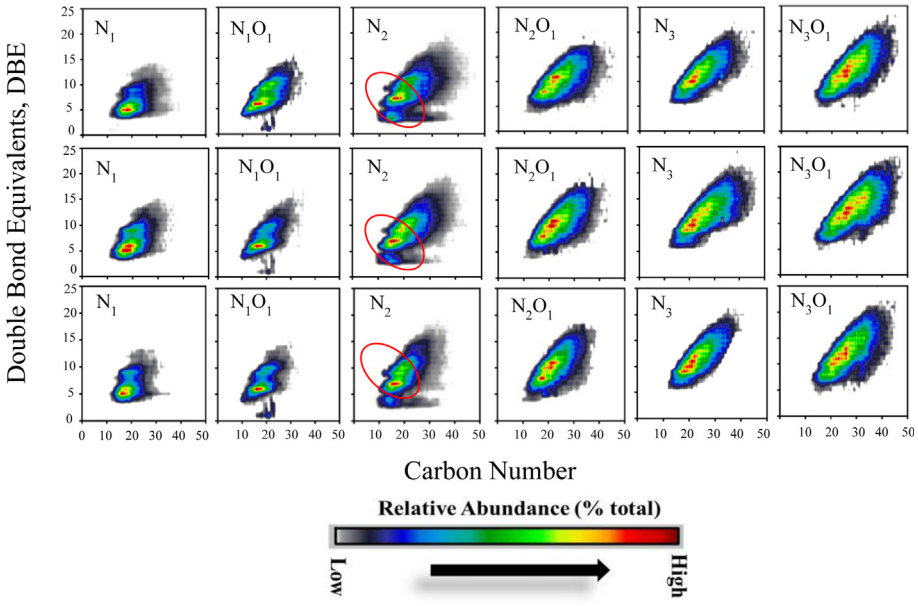

Fig. 5. Comparison of (+) ESI abundance-contoured plots of DBE versus carbon number for the biocrude oils produced at 300 °C from *C. merolae* (top), *G. sulphuraria* oils (middle) and co-liquefied biocrude produced at Q (bottom).

allows nonpolar sulfur speciation of complex petroleum mixtures (Purcell et al., 2006). Biocrude oils produced by individual HTL and co-liquefied HTL were analyzed by APPI FT-ICR MS technique to identify nonpolar to less polar compounds. Abundant heteroatom classes observed in the APPI positive-ion mode were hydrocarbons (HC), N_1 and O_1. Fig. 6 corresponds to the abundance-contour plots of DBE vs carbon number for the $[HC]^+$ + [HC]-Radical class for the biocrude oils produced by individual- and co-liquefaction

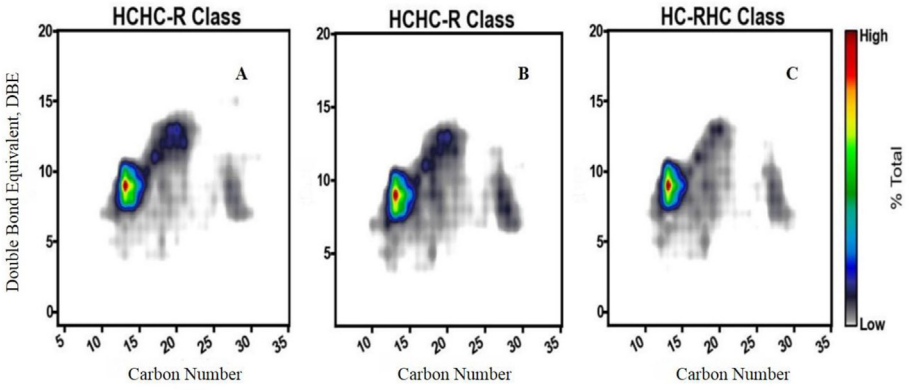

Fig. 6. Comparison of bio-crude oils by APPI FT-ICR MS; Top left (A), Biocrude oil from *C. merolae* at 300 °C; middle (B), biocrude oil from *G. sulphuraria* at 300 °C; Right (C), co-liquefied biocrude oil produced at Q.

of *C. merolae* and *G. sulphuraria*. The $[HC]^+$ + [HC]-Radical class species show compounds with 3–15 DBE and carbon content of ~10–30 atoms for all the three liquefied biocrude oils. This suggests the presence of hydrocarbons with a wide distribution of alkyl side chains. Since, this was the first APPI analysis approach on microalgal HTL biocrude oils the literature for comparison was limited. However, the chemical complexity of HTL biocrude resembles petroleum crude and current results are similar to Cho et al. (2012), Giraldo-Dávila et al. (2016). The region of highest abundance for all the three oils was located at DBE = 8–9 and carbon number 13. Therefore, mixing of two different microalgal species during co-liquefaction did not affect the molecular composition of the biocrude oils as analyzed by APPI FT-ICR MS.

4. Conclusions

Low lipid microalga *C. merolae* and *G. sulphuraria* were liquefied individually- and co-liquefied under subcritical water conditions. A maximum biocrude yield of 18.9 and 14.0% (based on dry weight) was achieved at 300 °C during individual liquefaction of *C. merolae* and *G. sulphuraria*, respectively. A biocrude oil yield of 25.88% was achieved when *C. merolae-G. sulphuraria* were co-liquefied at a mass loading ratio of 80–20%. The analysis and comparison of individual-, and co-liquefied biocrude performed by FT-ICR MS indicate that they were compositionally similar as indicated by their similar heteroatom class distribution and the observed similar carbon number and DBE distributions for the primary compounds in the biocrude.

Acknowledgements

This project was partially supported by U.S. Department of Energy (DE-EE0003046, DE-EE0006316) and National Science Foundation (EEC-1028968, IIA-130146).

References

Anastasakis, K., Ross, A., 2011. Hydrothermal liquefaction of the brown macro-alga Laminaria saccharina: effect of reaction conditions on product distribution and composition. Bioresour. Technol. 102 (7), 4876–4883.
Andersen, R.A., 2005. Algal Culturing Techniques. Academic Press.
Biller, P., Ross, A., 2011. Potential yields and properties of oil from the hydrothermal liquefaction of microalgae with different biochemical content. Bioresour. Technol. 102 (1), 215–225.
Bobleter, O., 1994. Hydrothermal degradation of polymers derived from plants. Prog. Polym. Sci. 19 (5), 797–841.
Brown, T.M., Duan, P., Savage, P.E., 2010. Hydrothermal liquefaction and gasification of Nannochloropsis sp. Energy Fuels 24 (6), 3639–3646.
Chen, W.-T., Zhang, Y., Zhang, J., Schideman, L., Yu, G., Zhang, P., Minarick, M., 2014. Co-liquefaction of swine manure and mixed-culture algal biomass from a wastewater treatment system to produce bio-crude oil. Appl. Energy 128, 209–216.
Chiaberge, S., Leonardis, I., Fiorani, T., Cesti, P., Reale, S., Angelis, F.D., 2014. Bio-oil from waste: a comprehensive analytical study by soft-ionization FTICR mass spectrometry. Energy Fuels 28 (3), 2019–2026.
Cho, Y., Na, J.-G., Nho, N.-S., Kim, S., Kim, S., 2012. Application of saturates, aromatics, resins, and asphaltenes crude oil fractionation for detailed chemical characterization of heavy crude oils by Fourier transform ion cyclotron resonance mass spectrometry equipped with atmospheric pressure photoionization. Energy Fuels 26 (5), 2558–2565.
Christensen, E., Sudasinghe, N., Dandamudi, K.P.R., Sebag, R., Schaub, T., Laurens, L. M., 2015. Rapid analysis of microalgal triacylglycerols with direct-infusion mass spectrometry. Energy Fuels 29 (10), 6443–6449.
Demirbas, A., 2010. Use of algae as biofuel sources. Energy Convers. Manage. 51 (12), 2738–2749.
Faeth, J.L., Savage, P.E., 2016. Effects of processing conditions on biocrude yields from fast hydrothermal liquefaction of microalgae. Bioresour. Technol. 206, 290–293.
Garcia Alba, L., Torri, C., Samorì, C., van der Spek, J., Fabbri, D., Kersten, S.R., Brilman, D.W., 2011. Hydrothermal treatment (HTT) of microalgae: evaluation of the process as conversion method in an algae biorefinery concept. Energy Fuels 26 (1), 642–657.
Giraldo-Dávila, D., Chacón-Patiño, M.L., Orrego-Ruiz, J.A., Blanco-Tirado, C., Combariza, M.Y., 2016. Improving compositional space accessibility in (+) APPI FT-ICR mass spectrometric analysis of crude oils by extrography and column chromatography fractionation. Fuel 185, 45–58.
Godwin, C.M., Hietala, D.C., Lashaway, A.R., Narwani, A., Savage, P.E., Cardinale, B.J., 2017. Algal polycultures enhance coproduct recycling from hydrothermal liquefaction. Bioresour. Technol. 224, 630–638.
Ikenaga, N.-O., Ueda, C., Matsui, T., Ohtsuki, M., Suzuki, T., 2001. Co-liquefaction of micro algae with coal using coal liquefaction catalysts. Energy Fuels 15 (2), 350–355.
Jin, B., Duan, P., Xu, Y., Wang, F., Fan, Y., 2013. Co-liquefaction of micro-and macroalgae in subcritical water. Bioresour. Technol. 149, 103–110.
Laurens, L.M., Dempster, T.A., Jones, H.D., Wolfrum, E.J., Van Wychen, S., McAllister, J.S., Rencenberger, M., Parchert, K.J., Gloe, L.M., 2012. Algal biomass constituent analysis: method uncertainties and investigation of the underlying measuring chemistries. Anal. Chem. 84 (4), 1879–1887.
Muppaneni, T., Reddy, H.K., Selvaratnam, T., Dandamudi, K.P.R., Dungan, B., Nirmalakhandan, N., Schaub, T., Holguin, F.O., Voorhies, W., Lammers, P., 2017. Hydrothermal liquefaction of Cyanidioschyzon merolae and the influence of catalysts on products. Bioresour. Technol. 223, 91–97.
Patil, V., Tran, K.-Q., Giselrød, H.R., 2008. Towards sustainable production of biofuels from microalgae. Int. J. Mol. Sci. 9 (7), 1188–1195.
Pearce, M., Shemfe, M., Sansom, C., 2016. Techno-economic analysis of solar integrated hydrothermal liquefaction of microalgae. Appl. Energy 166, 19–26.
Purcell, J.M., Hendrickson, C.L., Rodgers, R.P., Marshall, A.G., 2006. Atmospheric pressure photoionization Fourier transform ion cyclotron resonance mass spectrometry for complex mixture analysis. Anal. Chem. 78 (16), 5906–5912.
Roberts, G.W., Fortier, M.-O.P., Sturm, B.S., Stagg-Williams, S.M., 2013. Promising pathway for algal biofuels through wastewater cultivation and hydrothermal conversion. Energy Fuels 27 (2), 857–867.
Ross, A., Biller, P., Kubacki, M., Li, H., Lea-Langton, A., Jones, J., 2010. Hydrothermal processing of microalgae using alkali and organic acids. Fuel 89 (9), 2234–2243.
Schaub, T.M., Hendrickson, C.L., Horning, S., Quinn, J.P., Senko, M.W., Marshall, A.G., 2008. High-performance mass spectrometry: Fourier transform ion cyclotron resonance at 14.5 Tesla. Anal. Chem. 80 (11), 3985–3990.
Selvaratnam, T., Pegallapati, A., Montelya, F., Rodriguez, G., Nirmalakhandan, N., Van Voorhies, W., Lammers, P., 2014. Evaluation of a thermo-tolerant acidophilic alga, Galdieria sulphuraria, for nutrient removal from urban wastewaters. Bioresour. Technol. 156, 395–399.

Selvaratnam, T., Pegallapati, A., Montelya, F., Rodriguez, G., Nirmalakhandan, N., Lammers, P.J., Van Voorhies, W., 2015. Feasibility of algal systems for sustainable wastewater treatment. Renewable Energy 82, 71–76.

Sudasinghe, N., Dungan, B., Lammers, P., Albrecht, K., Elliott, D., Hallen, R., Schaub, T., 2014. High resolution FT-ICR mass spectral analysis of bio-oil and residual water soluble organics produced by hydrothermal liquefaction of the marine microalga Nannochloropsis salina. Fuel 119, 47–56.

Toor, S.S., Rosendahl, L., Rudolf, A., 2011. Hydrothermal liquefaction of biomass: a review of subcritical water technologies. Energy 36 (5), 2328–2342.

Toor, S.S., Reddy, H., Deng, S., Hoffmann, J., Spangsmark, D., Madsen, L.B., Holm-Nielsen, J.B., Rosendahl, L.A., 2013. Hydrothermal liquefaction of Spirulina and Nannochloropsis salina under subcritical and supercritical water conditions. Bioresour. Technol. 131, 413–419.

Toplin, J., Norris, T., Lehr, C., McDermott, T., Castenholz, R., 2008. Biogeographic and phylogenetic diversity of thermoacidophilic cyanidiales in Yellowstone National Park, Japan, and New Zealand. Appl. Environ. Microbiol. 74 (9), 2822–2833.

Torri, C., Garcia Alba, L., Samori, C., Fabbri, D., Brilman, D.W., 2012. Hydrothermal treatment (HTT) of microalgae: detailed molecular characterization of HTT oil in view of HTT mechanism elucidation. Energy Fuels 26 (1), 658–671.

Valdez, P.J., Nelson, M.C., Wang, H.Y., Lin, X.N., Savage, P.E., 2012. Hydrothermal liquefaction of Nannochloropsis sp.: systematic study of process variables and analysis of the product fractions. Biomass Bioenergy 46, 317–331.

Wang, L., Min, M., Li, Y., Chen, P., Chen, Y., Liu, Y., Wang, Y., Ruan, R., 2010. Cultivation of green algae Chlorella sp. in different wastewaters from municipal wastewater treatment plant. Appl. Biochem. Biotechnol. 162 (4), 1174–1186.

Wang, J., Krishna, R., Yang, J., Dandamudi, K.P.R., Deng, S., 2015. Nitrogen-doped porous carbons for highly selective CO_2 capture from flue gases and natural gas upgrading. Mater. Today Commun. 4, 156–165.

Williams, P.J.l.B., Laurens, L.M., 2010. Microalgae as biodiesel & biomass feedstocks: review & analysis of the biochemistry, energetics & economics. Energy Environ. Sci. 3 (5), 554–590.

Xu, L., Weathers, P.J., Xiong, X.R., Liu, C.Z., 2009. Microalgal bioreactors: challenges and opportunities. Eng. Life Sci. 9 (3), 178–189.

Yang, L., Li, Y., Savage, P.E., 2016. Near-and supercritical ethanol treatment of biocrude from hydrothermal liquefaction of microalgae. Bioresour. Technol. 211, 779–782.

Yu, G., Zhang, Y., Schideman, L., Funk, T., Wang, Z., 2011. Hydrothermal liquefaction of low lipid content microalgae into bio-crude oil. Trans. ASABE 54 (1), 239–246.

Zhang, L., Xu, C.C., Champagne, P., 2010. Overview of recent advances in thermo-chemical conversion of biomass. Energy Convers. Manage. 51 (5), 969–982.

Zhou, D., Zhang, L., Zhang, S., Fu, H., Chen, J., 2010. Hydrothermal liquefaction of macroalgae Enteromorpha prolifera to bio-oil. Energy Fuels 24 (7), 4054–4061.